Soil Microbial Community Responses to Additions of Organic Carbon Substrates and Heavy Metals (Pb and Cr)

Cindy H. Nakatsu,[1]* Nadia Carmosini,[1,2] Brett Baldwin,[1] Federico Beasley,[1]
Peter Kourtev,[2] and Allan Konopka[2]

Department of Agronomy[1] and Department of Biological Sciences,[2] Purdue University, West Lafayette, Indiana 47907

Microcosm experiments were conducted with soils contaminated with heavy metals (Pb and Cr) and aromatic hydrocarbons to determine the effects of each upon microbial community structure and function. Organic substrates were added as a driving force for change in the microbial community. Glucose represented an energy source used by a broad variety of bacteria, whereas fewer soil species were expected to use xylene. The metal amendments were chosen to inhibit the acute rate of organic mineralization by either 50% or 90%, and lower mineralization rates persisted over the entire 31-day incubation period. Significant biomass increases were abolished when metals were added in addition to organic carbon. The addition of organic carbon alone had the most significant impact on community composition and led to the proliferation of a few dominant phylotypes, as detected by PCR-denaturing gradient gel electrophoresis of bacterial 16S rRNA genes. However, the community-wide effects of heavy metal addition differed between the two carbon sources. For glucose, either Pb or Cr produced large changes and replacement with new phylotypes. In contrast, many phylotypes selected by xylene treatment were retained when either metal was added. Members of the *Actinomycetales* were very prevalent in microcosms with xylene and Cr(VI); gene copy numbers of biphenyl dioxygenase and phenol hydroxylase (but not other oxygenases) were elevated in these microcosms, as determined by real-time PCR. Much lower metal concentrations were needed to inhibit the catabolism of xylene than of glucose. Cr(VI) appeared to be reduced during the 31-day incubations, but in the case of glucose there was substantial microbial activity when much of the Cr(VI) remained. In the case of xylene, this was less clear.

The use and release of heavy metals to air, water, and soils has created a significant number of contaminated sites across the United States and the world. Thus, the effect of metal contamination on the microbial community has been extensively studied over the past several decades. The acute effects of short-term exposure to toxic heavy metals upon a broad array of microbial processes have been well documented (9, 10, 21, 40, 47). More recently, investigators have examined habitats exposed to anthropogenic or natural metal contamination over an extended period of time (5, 20, 22, 24, 39, 45). Studies that focused on the culturable fraction of the microbial community indicated that as few as 10 to almost 100% of the bacteria in habitats contaminated for extended periods were metal resistant. Thus, there may be substantial variability in community responses to metal exposure between locations. As non-cultivation-based methods have become available, researchers have begun examining the impact of metal exposure on the entire indigenous community (6, 24, 25, 26) and have tried to address the impact of these exposures on community diversity (30) and resiliency (15).

A confounding factor in metal-contaminated sites is the frequent co-occurrence of organic contaminants. These organic molecules may be metabolizable energy sources, toxicants, or both. The combined effect of metals and organic carbon pollutants on microbial activity and community composition is unclear since no studies have addressed this point. If species richness is reduced in sites contaminated with complex mixtures, the communities may be less resilient because the probability that an ecotype is capable of a specific required function is reduced (13). Previous research in our laboratory showed that the microbial community structure in a long-term mixed-waste contaminated site might reflect both metal and aromatic hydrocarbon concentrations in the soil. For individual microbes to persist under complex conditions, they must tolerate both local metal and hydrocarbon contaminants. Shi et al. (42) found a very broad distribution of metal tolerances within the microbial communities in these soils. This is consistent with a heterogeneous distribution of microbes in both highly contaminated and noncontaminated microsites.

For this study, we used microcosms to segregate the effects of two metals, Pb and Cr, and also to study the impact of aromatic hydrocarbons on microbial community structure and activity. By using microcosms, soils could be homogenized to evenly distribute both the microbial populations and toxicants and thereby reduce spatial variability. This allowed us to test experimental additions of Pb^{2+} or Cr^{6+} and to assess their effects on the microbial community. One of two energy substrates (glucose or xylene) was added to provide the necessary force for selection to operate and drive changes in community composition. Glucose is broadly utilized by microorganisms; xylene catabolism is more restricted among microbes, and xylene mimics aromatic compounds present in these soils. The changes in community activity were related to molecular analyses of community composition and functional gene levels.

* Corresponding author. Mailing address: Department of Agronomy, Purdue University, West Lafayette, IN 47907-2054. Phone: (765) 496-2997. Fax: (765) 496-2629. E-mail: cnakatsu@purdue.edu.

MATERIALS AND METHODS

Soil microcosms. Soils used for microcosm experiments were collected on 27 June 2001 from an Indiana Department of Transportation property in Seymour, Ind., which was contaminated with metals and petroleum hydrocarbons (21a). The soils chosen for these microcosm experiments originated from a less contaminated area of the site; the total Pb and Cr levels were 20 and 6 mg kg^{-1} soil, respectively. Soil was stored at 4°C until 7 days prior to commencing the microcosm experiments, when it was transferred to 1-liter jars for acclimatization, which included daily soil mixing and aeration.

Soil microcosms consisted of 100-ml serum bottles containing 12 g dry weight of soil. A total of eight metal-carbon combinations and three control treatments were tested. The combinations included glucose or xylene with low or high Pb, glucose or xylene with low or high Cr, and control treatments with additions of glucose only, xylene only, and no addition of organic or metal. Xylene or glucose was added at a concentration of 3,000 μg per gram of soil. Preliminary experiments determined that carbon mineralization was maximized at this concentration. A sterilized glucose solution was added to the microcosms, whereas xylene was added to the soil by first mixing 418.6 μl of xylene to 10 g of sand and then adding 1 g of the xylene-sand mixture to each microcosm. To minimize volatilization, all xylene additions were done over dry ice. The soils were mixed manually to distribute the substrates as homogeneously as possible. The concentrations of metals were chosen to reduce substrate-induced carbon mineralization by 50% (L) and 90% (H). These concentrations were determined for each substrate in preliminary experiments. The L and H metal concentrations were 3 and 10 mg g^{-1} of Pb (corresponds to 36 and 122 mmol kg^{-1}) with glucose or xylene, 0.4 and 4 mg g^{-1} of Cr(VI) (corresponds to 16 and 160 mmol kg^{-1}) with glucose, and 10 and 18 μg g^{-1} of Cr(VI) (corresponds to 0.4 and 0.7 mmol kg^{-1}) with xylene. Solutions of Pb as Pb(NO$_3$)$_2$ and of Cr(VI) as K$_2$CrO$_4$ were evenly dispersed in microcosms. The final moisture concentration of each microcosm was adjusted to a 60% water-holding capacity; the adjustments were made after measuring the water-holding capacity of the soil, as described previously (11). The microcosms were then sealed. They were weighed every week to check that the moisture content remained at the same level.

Three microcosms were destructively sampled on days 0, 4, 7, 10, 13, 16, 20, 25, and 31 for CO$_2$, total biomass (phospholipid phosphates), and soil DNA measurements. First, 0.5 ml of headspace gas was removed from each microcosm by use of a syringe and injected into a gas chromatograph (HP series II 5890) to measure the CO$_2$ content. Numbers of cultivable Cr-resistant and xylene-degrading bacteria were immediately estimated from the xylene-plus-high-Cr microcosms, using 1 g of soil. For microcosms that received Cr(VI), 1 g of soil was extracted with water, and the amount of soluble Cr(VI) was determined spectrophotometrically using the diphenylcarbazide assay (12). For microbial community analysis, 2 g of soil was placed in a microcentrifuge tube and frozen until DNA could be extracted. The remaining soil was stored in a small ziplock bag and frozen for biomass (phospholipid-PO$_4$) and fatty acid methyl ester analyses.

Phospholipid analysis. Phospholipids were extracted using the method of Findlay (16). Extractions were done in triplicate with 10 g of soil. Total lipid was extracted from the soils using a methanol-chloroform-phosphate buffer (1:2:0.8), and phospholipids were fractionated by column chromatography. The microbial biomass was estimated from the phospholipid-PO$_4$ content of the soil. A 100-μl portion of the phospholipid extract was used to determine the amount of phospholipid-PO$_4$ after potassium persulfate digestion by use of a colorimetric assay (1).

Enumeration of cultivable bacteria. Total cultivable bacteria and those that were Cr resistant were enumerated from 1 g (wet mass) soil from the xylene-plus-high-Cr microcosms on days 0 (prior to the addition of xylene and Cr), 4, 7, 10, 13, 16, 20, 25, and 31. Soils were first suspended in 10 ml of xenobiotic basal salts medium (23) and vortexed. Serial dilutions (10^{-2} to 10^{-5}) of the soil suspension were made, and 100-μl samples were plated in triplicate onto xenobiotic basal salts agar plates with xylene plus 1 mM K$_2$CrO$_4$ and onto 0.1× nutrient agar (NA) plates with and without the addition of 5 mM K$_2$CrO$_4$. Xylene was supplied as a vapor saturating the atmosphere of the enclosure used to incubate the plates. The number of colonies was counted after 4 or 7 days of incubation at 25°C.

DNA extraction, PCR, and denaturing gradient gel electrophoresis (DGGE). Soil DNAs from approximately 0.5 g of soil were extracted using a FastDNA spin kit for soil (QBIOgene, Carlsbad, CA) according to the manufacturer's instructions. The resolution of extracts in a 0.7% agarose gel containing ethidium bromide (0.3 μg ml^{-1}) was used to estimate the DNA quantity and quality.

Changes in the microbial community of the microcosms were followed over time by DGGE of PCR products from 16S rRNA genes as previously described (31, 33). Briefly, the V3 region of the 16S rRNA gene was amplified by using primer PRBA338f (5′ AC TCC TAC GGG AGG CAG CAG 3′) (32) with a GC

clamp (5′-CGC CCG CCG CGC GCG GCG GGC GGG GCG GGG GCA CGG GGG G-3′) attached to the 5′ end and primer PRUN518r (5′-ATT ACC GCG GCT GCT GG-3′) (27). PCR mixtures contained 1× PCR buffer (Promega, Madison, WI), 3.5 mM MgCl$_2$, 0.8 μmol of each deoxynucleoside triphosphate, 0.1% bovine serum albumin, 0.5 μM (each) forward and reverse primers, 5 U of *Taq* polymerase, and 1 to 50 ng of template DNA. Amplification was performed by 5 min of denaturation at 94°C and then 30 cycles of 30 s each at 92°C, 55°C, and 72°C, followed by a final extension at 72°C for 15 min using a PTC-100 thermal cycler (MJ Research Inc., Watertown, MA). PCR products were confirmed in a 1.0% agarose gel containing ethidium bromide (0.3 μg ml^{-1}); the fluorescence intensity was used to estimate their quantities.

For DGGE, equivalent quantities of PCR products were resolved in an 8% (wt/vol) polyacrylamide gel (37.5:1 acrylamide:bisacrylamide) in 0.5× TAE (20 mM Tris-HCl, 10 mM acetate, 0.5 mM EDTA) and denaturants (100% denaturant contains 7 M urea and 40% deionized formamide). A gradient of denaturants ranging from 35% to 58% was used to compare communities. Narrower gradients (35 to 45% or 45 to 58%) were used to resolve putative doublets. Electrophoresis was performed on a D-Gene apparatus (Bio-Rad, Hercules, CA) at a constant voltage of 20 V for 15 min, followed by 200 V for 5.5 h. After electrophoresis, gels were stained with SYBR green I (Cambrex Bio Science, Rockland, ME) and then photographed with a Polaroid camera (Cambridge, MA).

Statistical analysis. Profiles generated by PCR-DGGE were analyzed using the BioNumerics program (Applied Maths, Belgium). Comparisons were made between each fingerprint from the microcosm samples collected over time. The program uses binary data based on the presence or absence of each band in the fingerprint profile pairs being compared. The phospholipid fatty acid results were analyzed using a similar approach (Star Chromatography Workstation software; Varian Inc.). Community similarities based on DGGE bands were then quantified by principal component analysis (36) using BioNumerics software.

Multiplex PCR. Microcosm soil samples were initially screened for aromatic oxygenase genes using previously described PCR primers and multiplex PCR protocols (7). This method was also used to screen all isolates cultivated from the microcosms. Briefly, individual primer sets were used to amplify portions of the naphthalene dioxygenase, toluene dioxygenase (TOD), toluene monooxygenase, ring-hydroxylating toluene monooxygenase (RMO), phenol hydroxylase (PHE), and biphenyl dioxygenase (three different primer sets [for BPH1, BPH2, and BPH4]) genes. All PCR experiments included reaction mixtures with DNA extracts from appropriate positive control strains and mixtures containing no template. The positive controls used were as follows: for naphthalene dioxygenase, *Pseudomonas putida* G7; for TOD, *Pseudomonas putida* F1; for toluene monooxygenase, *Pseudomonas putida* HS1; for RMO, *Pseudomonas aeruginosa* JI104; for PHE, *Pseudomonas* sp. strain CF600; for BPH1, *Comamonas testosteroni* B-356; for BPH2, *Pseudomonas pseuodoalcaligenes* KF707; and for BPH4, *Rhodococcus* sp. strain RHA1. PCR products were routinely visualized by running 10 μl of PCR mixture in 1% agarose gels (Bio-Rad, Richmond, CA) in 1× Tris-acetate-EDTA (41) with ethidium bromide (0.3 μg ml^{-1}) staining.

Real-time quantitative PCR with SYBR green I. Genes that were detected in the initial PCR screen were quantified by real-time PCR using samples collected on days 0, 16, and 25 of the microcosm experiment. Real-time PCR was performed on an ABI 7700 Sequence Detector instrument (version 1.7 software; Applied Biosystems, Foster City, CA). Quantitative PCR mixtures contained 1× cloned *Pfu* buffer, 1 U *Pfu*Turbo HotStart DNA polymerase (Stratagene, La Jolla, CA), a 0.2 mM concentration of each deoxynucleoside triphosphate, SYBR green I (1:30,000; Cambrex Bio Science, Rockland, ME), and MgCl$_2$ at a concentration optimized for each primer set. Annealing and polymerization temperatures, primer concentrations, and MgCl$_2$ concentrations for real-time PCR were the same as those described previously (5). Calibration curves for each target were made with standards during each real-time PCR experiment. The full-strength extract and a 1:10 dilution of all environmental samples were analyzed in duplicate. The Sequence Detector software subtracted the background signal for each sample determined in cycles 3 through 15. The fluorescence threshold was defined as 10 times the standard deviation of the background signal. The threshold cycle (C_T) was defined as the fractional cycle number in which the signal exceeded the fluorescence threshold. The computed threshold cycle inversely correlated with the log of the initial template concentration. The best fit (by the method of least squares) was then used to plot the standard curve. The lower detection limit was defined as the lowest template concentration that resulted in a threshold cycle that was significantly less than the total number of cycles performed ($\alpha = 0.05$).

Nucleotide sequence determination. The nucleotide sequences of select bands from DGGE profiles using the DGGE primers listed above were also determined (28, 32). Bands from day 31 of the xylene-plus-high-Cr(VI) treatment were targeted, as were the strong bands that arose in response to glucose alone.
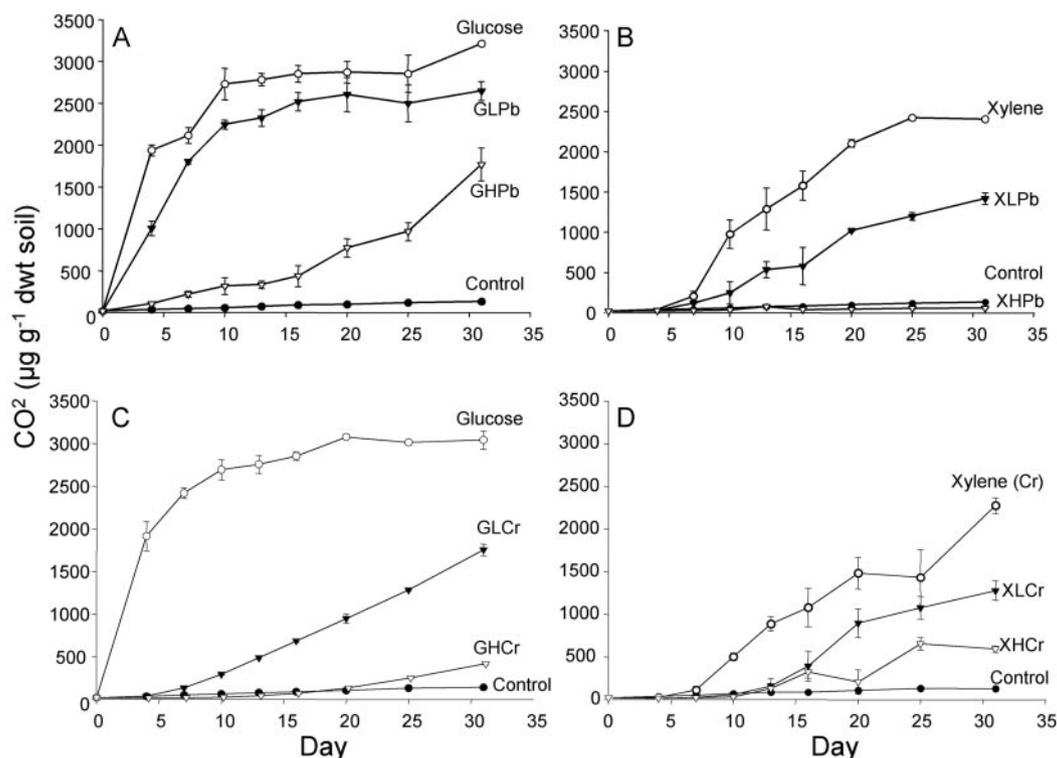
FIG. 1. Cumulative carbon mineralization of microcosms amended with glucose and lead (A), xylene and lead (B), glucose and chromate (C), and xylene and chromate (D). Treatment microcosms received 3,000 $\mu g\ g^{-1}$ of either glucose or xylene with low lead (LPb) at 3,000 $\mu g\ Pb^{2+}\ g^{-1}$ soil or high lead (HPb) at 10,000 $\mu g\ g^{-1}$, glucose with low chromium at 400 $\mu g\ Cr^{6+}\ g^{-1}$ soil (GLCr) or high chromium at 4,000 $\mu g\ Cr^{6+}\ g^{-1}$ (GHCr), or xylene with low chromium at 10 $\mu g\ Cr^{6+}\ g^{-1}$ soil (XLCr) or high chromium at 18 $\mu g\ Cr^{6+}\ g^{-1}$ (XHCr). dwt, dry weight.

Reagents and conditions for PCR were used as previously described (28). Sequences of specific DGGE bands were determined by excision of the band, elution in sterilized PCR water, reamplification with primers 341-f and 534-r (without the GC clamp), and cloning of the amplicons into the pGEM-T Easy cloning vector (Promega, Madison, WI). Nucleotide sequences were determined using a Thermo Sequenase cycle sequencing kit (Amersham Pharmacia Biotech, Piscataway, NJ) and an ALFexpress automated sequencer (Amersham Pharmacia Biotech). For all amplicons, the sequence was analyzed in both the forward and reverse directions, and in most cases two clones were sequenced for each excised band. Nucleotide sequences were compared to sequences in the National Center for Biotechnology Information GenBank database by using the BLASTn program (2).

Nucleotide sequence accession numbers. The nucleotide sequences obtained in this study have been deposited in the GenBank database under accession no. DQ016373 to DQ016386.

RESULTS

Microbial activity. The effects of carbon and metal amendments on community activity provide a context for examining the dynamics of community composition. The addition of organic C alone (either glucose or xylene) stimulated carbon mineralization in the microcosms (Fig. 1). In the case of xylene, there was a lag period of about 7 days before CO_2 accumulation was detected, and a smaller proportion of added organic C was mineralized. For glucose, cumulative CO_2 levels reached a plateau at 70% of the theoretical maximum mineralization of 4,400 $\mu g\ CO_2\ g^{-1}$ soil, whereas for xylene only 25% of the theoretical maximum mineralization of 10,000 $\mu g\ CO_2\ g^{-1}$ soil was observed. It is indeterminate if this was due to the formation of bound residues in the soil or to volatilization losses in

the microcosm. However, the experiment was designed to compare these treatments to those with added metals.

The level of added metals was chosen to reduce the short-term (2 days for glucose and 7 days for xylene) substrate-induced carbon mineralization response by 50% or 90% and then examine the adaptive response of the microbial community over a 31-day period. Note that lower levels of Cr(VI) than Pb were added to inhibit carbon mineralization and that in the case of Cr(VI), at least 40-fold lower concentrations inhibited xylene catabolism than glucose mineralization. The mineralization rates were reduced when metals were added, as expected. If a metal-tolerant adapted population proliferated early in the incubation, a second phase of faster mineralization (at least at the rate seen for microcosms without metal additions) might be expected. However, this was not observed and the rates were constant over the incubation period, with the possible exception of the microcosms with glucose and a high Pb concentration. In general, the addition of either low or high levels of Cr(VI) resulted in extended lag periods beyond those for treatments without heavy metals or those to which Pb was added.

Relationship of Cr(VI) reduction to C mineralization. Mineralization increased in the glucose–low-Cr microcosms at a time when 24% of the added Cr(VI) had been reduced (Fig. 2, bottom left panel). However, there was substantial mineralization (60 $\mu g\ CO_2\ g\ soil^{-1}\ day^{-1}$) at Cr(VI) levels of 200 to 250 $\mu g\ g^{-1}$ soil. In the glucose–high-Cr microcosms, glucose mineralization occurred at Cr(VI) levels above 3,000 $\mu g\ g^{-1}$ for the first 25 days, and Cr(VI) reduction was only detected after
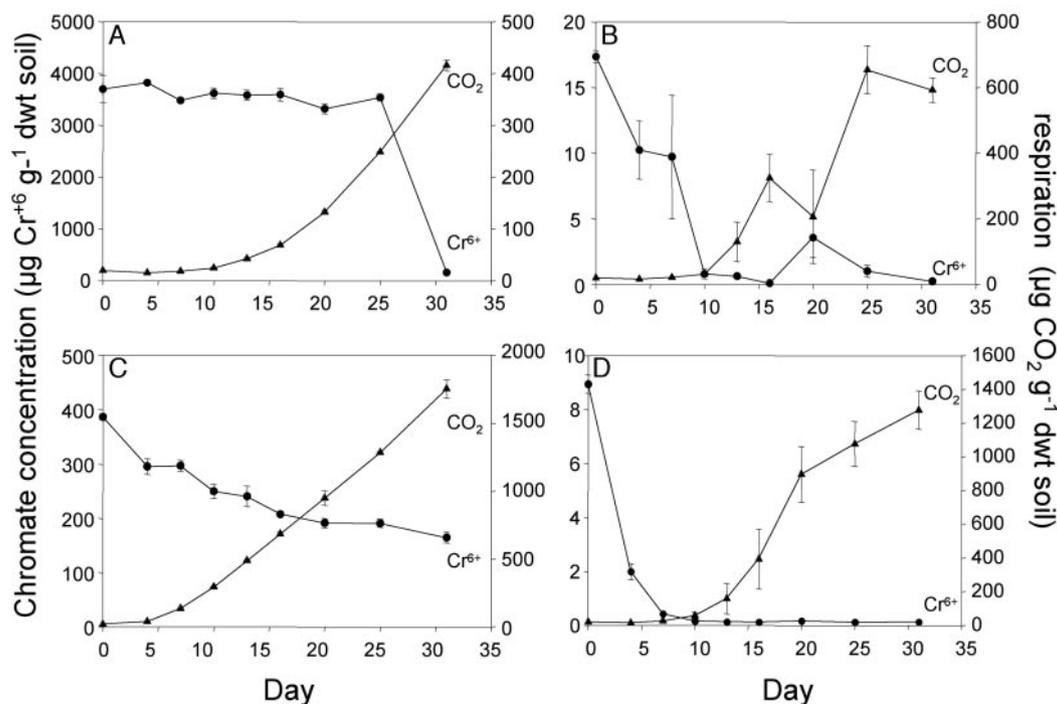
FIG. 2. Comparison of chromium reduction and carbon mineralization by measuring concentrations of Cr^{6+} and cumulative CO_2 in soil microcosms amended with glucose plus 4,000 μg Cr^{6+} g^{-1} soil (A), xylene plus 18 μg Cr^{6+} g^{-1} soil (B), glucose plus 400 μg Cr^{6+} g^{-1} soil (C), and xylene plus 10 μg Cr^{6+} g^{-1} soil (D). Treatment microcosms received 3,000 μg g^{-1} of either glucose or xylene.

25 days of incubation (Fig. 2, top left panel). In contrast, in the xylene-Cr microcosms, a substantial reduction in Cr(VI) preceded the onset of detectable carbon mineralization (Fig. 2, right panels). In xylene–low-Cr microcosms, xylene mineralization was not detected until 6 days after Cr(VI) had disappeared. In the xylene–high-Cr microcosms, Cr(VI) had been reduced by 98% by day 10, and carbon mineralization did not increase above background levels until day 13.

Microbial biomass. Microbial biomass synthesis appeared to be decoupled from microbial activity when metal stresses were imposed. When only glucose was added, threefold increases in phospholipid-phosphate were detected in 4 days (Fig. 3). There was always a lag period in xylene metabolism, but the biomass increased above background levels within 10 to 13 days in microcosms that received xylene but no metals. In contrast, biomasses for glucose–high-Pb, xylene–low-Pb, glucose–low-Cr, xylene–low-Cr, and xylene–high-Cr treatments remained similar to or below background levels throughout the 31 days, even though microbial activity (carbon mineralization) was occurring. The only metal treatment for which a net biomass increase was observed was the twofold increase found when glucose and a low level of Pb were added (Fig. 3).

Culturable bacteria. Our analysis focused on the microcosms with aromatic substrate (xylene) and high Cr(VI) additions because of reports that heavy metals appeared to restrict the occurrence of aromatic-degrading bacteria (49). Throughout the experiment, no colonies formed on plates containing xylene plus 1 mM Cr. Total culturable heterotrophic bacteria increased from 10^5 CFU per g soil on day 0 to about 10^6 on day 10 and increased another 10-fold by day 20 (Fig. 4). The number of bacteria resistant to 5 mM chromate was below the detection limit of 3,000 g^{-1} until day 10. The selection of isolates at 5 mM chromate is relatively severe, and this concentration is probably higher than the in situ concentration with a Cr(VI) addition of 18 μg Cr(VI) g^{-1} soil. The proportion of Cr-resistant bacteria increased from days 10 to 16 and then declined. However, highly chromium-resistant bacteria always comprised <10% of all cultivatable bacteria. The increase in CFU of total and Cr-resistant bacteria corresponded with the increase in carbon mineralization and also with the decrease in Cr(VI) concentration.

Community profiling by DGGE. A subset of PCR-DGGE fingerprints that were analyzed from the various microcosms is illustrated in Fig. 5. Visual inspection of the PCR-DGGE gels indicated a smear of bands in the background of each profile, and some bands had notably greater intensities. Bands of greater intensity were more commonly found in samples where substantial microbial activity had been detected. For example, they were not observed in the xylene–high-Pb microcosms at any time and were observed in the glucose–high-Cr microcosms on day 31 only, when carbon mineralization exceeded that in the unamended control. Profiles with intense bands did have one band in common (Fig. 5, arrowheads). We presume that bands of greater intensity represent the populations that are most competitive under the selective conditions used. The lack of intense bands may result from the lack of a growth response or an equitable selection of a number of microbes such that no one or two become predominant.

With the exception of those of the xylene microcosms, the fingerprints from the replicate microcosms sampled on the
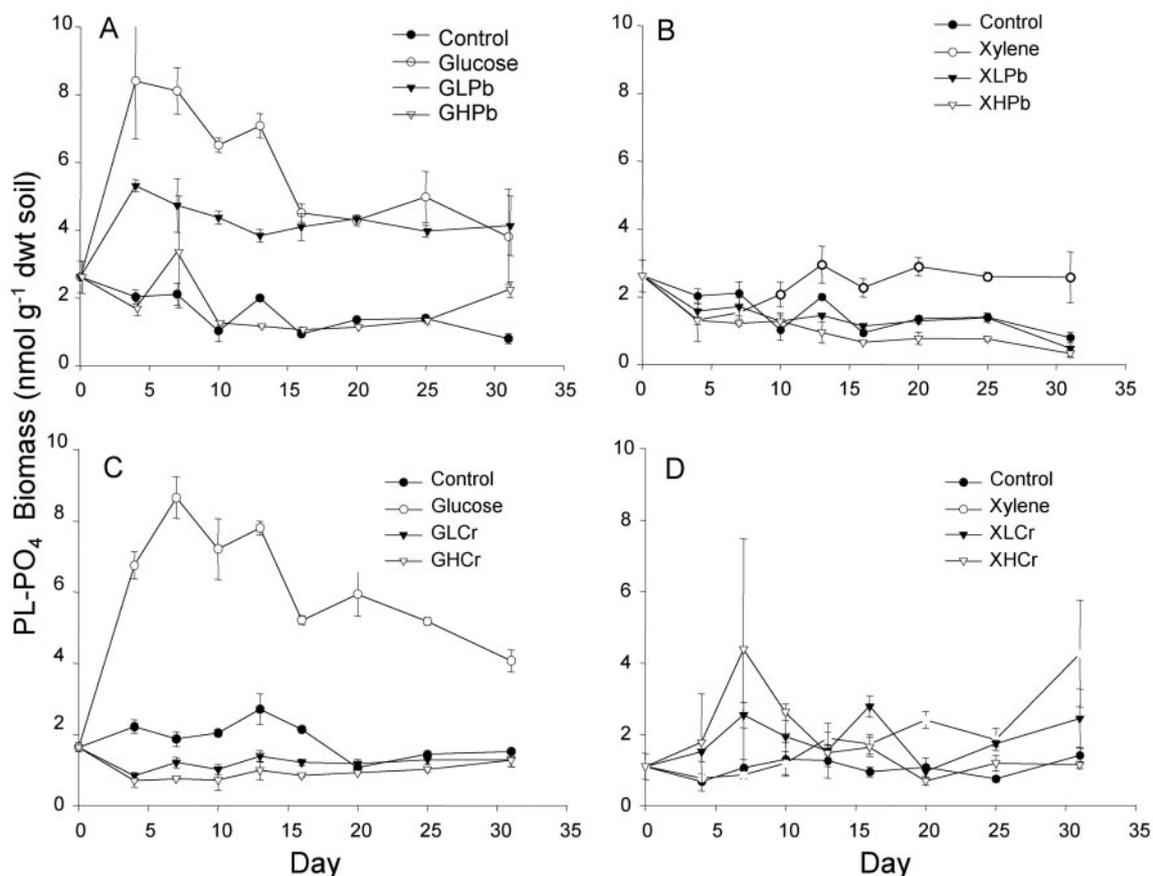
FIG. 3. Phospholipid-phosphate biomass in soil microcosms amended with glucose and lead (A), xylene and lead (B), glucose and chromate (C), and xylene and chromate (D). Treatment microcosms received 3,000 $\mu g\ g^{-1}$ of either glucose or xylene with low lead (LPb) at 3,000 $\mu g\ Pb^{2+}$ g^{-1} soil or high lead (HPb) at 10,000 $\mu g\ g^{-1}$, glucose with low chromium at 400 $\mu g\ Cr^{6+}\ g^{-1}$ soil (GLCr) or high chromium at 4,000 $\mu g\ Cr^{6+}\ g^{-1}$ (GHCr), or xylene with low chromium at 10 $\mu g\ Cr^{6+}\ g^{-1}$ soil (XLCr) or high chromium at 18 $\mu g\ Cr^{6+}\ g^{-1}$ (XHCr).
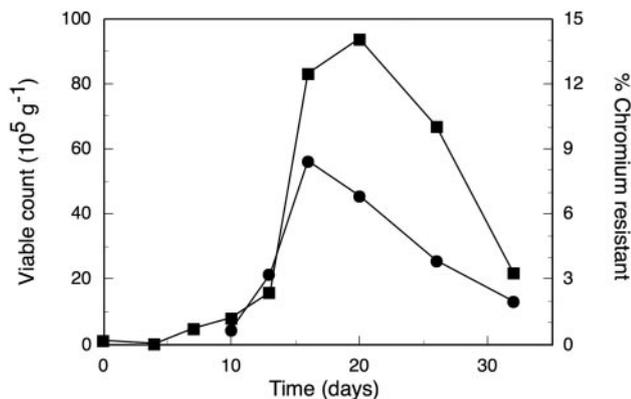

FIG. 4. Number of cultivable bacteria in microcosms that received 3,000 $\mu g\ g^{-1}$ of xylene and high chromium at 18 $\mu g\ Cr^{6+}\ g^{-1}$. ■, total number of CFU ($10^5\ g^{-1}$) on dilute nutrient agar. Samples were also plated on dilute nutrient agar plus 1 mM K_2CrO_4, and the viable counts on this medium are expressed as percentages of that on medium without K_2CrO_4 (●). For days 0, 4, and 7, the numbers of chromium-resistant bacteria were less than the detection limit of 3×10^{-3}.

same date were highly reproducible, but there were occasional differences in band intensity (data not shown). Microcosms that received only an organic substrate were constructed at two distinct times, once as a control for Pb additions and the other as a control for Cr additions. In the case of xylene, variation among the three replicates was observed both times. For glucose microcosms, the fingerprints were the same for the six microcosms that comprised the two experiments. The similarities between the communities were best illustrated by multivariate statistical analysis. The addition of organic C alone caused substantial shifts in community composition, but the presence of heavy metals had significant impacts on these community shifts (Fig. 6). The two different C sources used (glucose and xylene) produced very different effects on microbial communities; these effects appeared larger than those caused by the addition of heavy metals (Fig. 7).

However, heavy metal addition did modulate the community response to organic carbon, and the nature of that modulation was correlated with the carbon substrate rather than the specific metal added. When glucose (a substrate that probably could be used by a wide range of microbes in the soil) was the driving force, the addition of Pb or Cr resulted in very substantial changes. In particular, most of the highly intense bands that arose in response to glucose alone were absent when
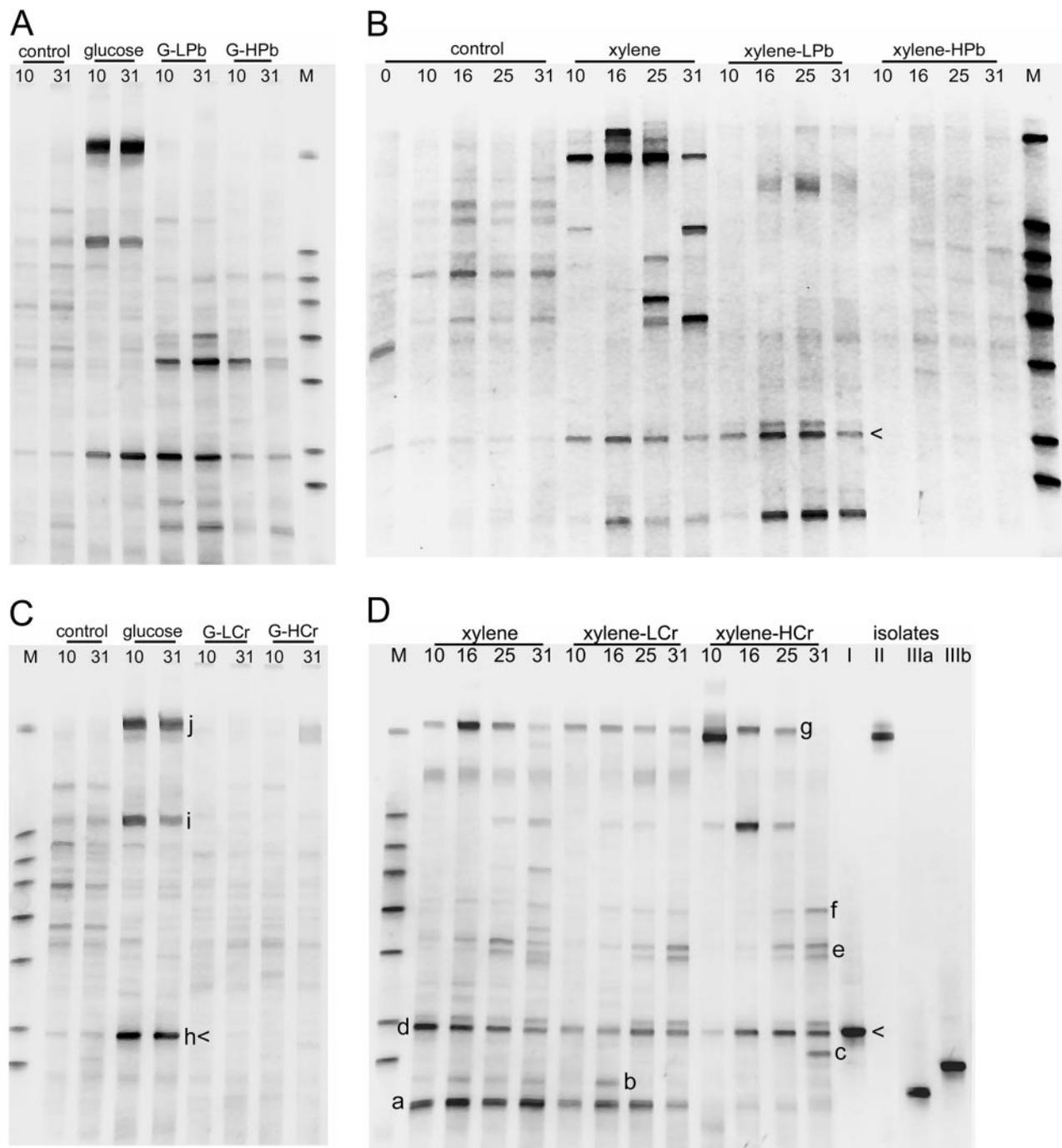
FIG. 5. Community profiles based on DGGE profiles of the V3 region of the 16S rRNA gene amplified by PCR from DNA extracts from microcosms amended with glucose and lead (A), xylene and lead (B), glucose and chromate (C), and xylene and chromate (D). The number above each lane represents the day the microcosm was sampled. G, glucose; L, low metal; H, high metal; M, markers used to normalize band mobilities between different gels. In panel D, the lanes marked I, II, IIIa, and IIIb indicate xylene-degrading bacterial isolates for which the best 16S rRNA gene sequence matches are as follows: I, *Arthrobacter* sp.; II, *Pseudomonas fluorescens*; and IIIa and IIIb, *Rhodococcus* sp. Arrowheads designate bands matching isolates from group I. Letters a to h and i to k designate bands that were excised and sequenced from gels from xylene and glucose microcosms, respectively. See Table 3 for the phylogenetic identities of these bands.

metals were also present (Fig. 5A and C). These were replaced by a number of other bands; phylotype richness did not appear to be diminished by the addition of heavy metals, but there was selection for different phylotypes. In contrast, the addition of

heavy metals to microcosms with xylene (a substrate that requires a specialized catabolic pathway) resulted in the retention of a number of phylotypes that responded to xylene alone (Fig. 5B and D). There was also the appearance of new phy-
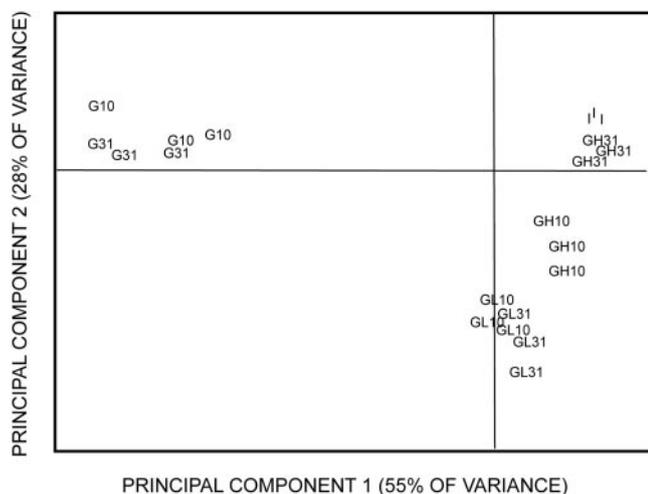
FIG. 6. Principal component analysis of PCR-DGGE profiles on days 10 and 31 for microcosms amended with glucose and lead. Treated microcosms received 3,000 $\mu g\ g^{-1}$ of glucose (G), low lead (L) at 3,000 $\mu g\ Pb^{2+}\ g^{-1}$ soil, or high lead (H) at 10,000 $\mu g\ g^{-1}$. I, samples analyzed on day 0, prior to amendments. There were three replicates tested for each treatment. The symbols denote the additions and the day of analysis (10 or 31 days).

lotypes or an intensification of minor phylotypes observed in the absence of metals.

Quantification of functional genes that respond to xylene. Of the eight oxygenases that were screened by PCR, only the biphenyl dioxygenase (BPH4) and phenol hydroxylase (PHE) genes were detected in xylene microcosms. They were found in all microcosms, with the exception of xylene–high-Pb microcosms, where no BPH4 or PHE genes were detected, and xylene–high-Cr microcosms, where the PHE gene was not de-
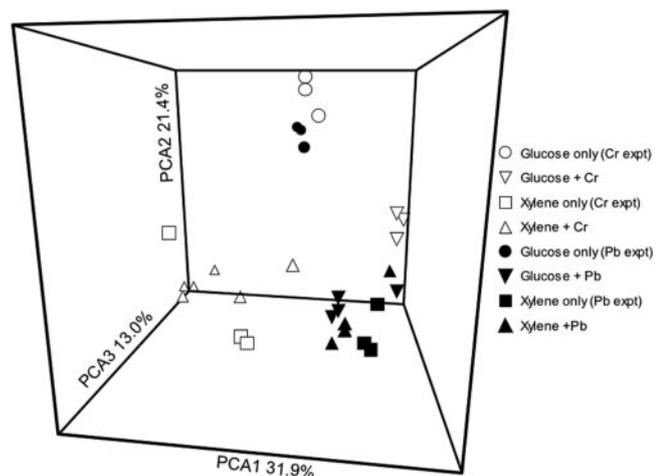

FIG. 7. Principal component analysis of PCR-DGGE profiles on day 31 for microcosm series that received either Cr (open symbols) or Pb (solid symbols). Treatment microcosms received 3,000 $\mu g\ g^{-1}$ of either glucose or xylene. The data for the two treatment levels of either Pb or Cr (low or high) were pooled. The experiments with additions of Pb or Cr were run at different times; therefore, two sets of control microcosms, to which carbon but not heavy metal was added (glucose only or xylene only), were analyzed, and both sets of controls are plotted.

tected (Tables 1 and 2). In microcosms with no substrate additions, gene copy numbers generally decreased or remained stable over the course of the experiment. An exception was the BPH4 gene in the control microcosms for the Cr treatments, where there was a twofold increase; however, this change was much smaller than the 7- to 60-fold increases in BPH4 and PHE gene copy numbers observed in response to xylene. Pb had a substantial impact on these functional activities. As noted above, gene copy numbers were below the detection limit for high Pb additions. With a low Pb concentration, the BPH4 gene number increased similarly to that in microcosms without Pb, but PHE copy numbers did not. PHE gene numbers were also adversely affected by the addition of Cr, whereas the BPH4 gene copy number increased with either low or high doses of Cr. It is indeterminate whether the selective effects of metals on PHE genes are direct consequences of toxic effects, specifically on an enzyme in this pathway, or are indirect in that the bacterial species containing these genes were more sensitive to Pb or Cr than those expressing BPH4.

TABLE 1. Estimation of BPH4 copy numbers using real-time PCR

Microcosm[c]	BPH4 copy no. (10^7 copies/g soil) on sampling day[d]		
	0	16	25
No substrate	2.5 (2.5)	0.9 (0.4)	0.5 (0.2)
Xylene	2.5 (2.5)	17.1 (15.4)[a,b]	7.9 (3.7)[a,b]
Xylene + LPb	2.5 (2.5)	10.5 (7.4)[a,b]	6.2 (2.9)[a,b]
Xylene + HPb	2.5 (2.5)	BD	BD
No substrate	3.4 (1.7)	5.1 (0.7)[a]	7.6 (2.3)[a]
Xylene	3.4 (1.7)	23.3 (11.8)[a,b]	32.3 (20.0)[a,b]
Xylene + LCr	3.4 (1.7)	16.3 (23.6)	9.5 (6.0)[a]
Xylene + HCr	3.4 (1.7)	17.2 (10.7)[a,b]	41.3 (15.8)[a,b]

[a] Significantly more copies than at time 0 ($P = 0.05$).
[b] Significantly more copies than measured in the no-substrate control microcosm at that time ($P = 0.05$).
[c] Treatment microcosms received 3,000 $\mu g\ g^{-1}$ of xylene, low lead (LPb) at 3,000 $\mu g\ Pb^{6+}\ g^{-1}$ soil, high lead (HPb) at 10,000 $\mu g\ g^{-1}$, low chromium at 10 $\mu g\ Cr^{6+}\ g^{-1}$ soil (LCr), or high chromium at 18 $\mu g\ Cr^{6+}\ g^{-1}$ (HCr).
[d] BD, below detection limit (200 copies per reaction mixture). Numbers in parentheses are standard deviations ($n = 3$).

TABLE 2. Estimation of PHE copy numbers using real-time PCR

Microcosm[c]	PHE copy no. (10^7 copies/g soil) on sampling day[d]		
	0	16	25
No substrate	0.6 (0.3)	0.5 (0.1)	0.6 (0.3)
Xylene	0.6 (0.3)	2.4 (0.7)[a,b]	19.6 (17.3)[a,b]
Xylene + LPb	0.6 (0.3)	0.4 (0.1)	0.5 (0.1)
Xylene + HPb	0.6 (0.3)	BD	BD
No substrate	0.5 (0.1)	0.2 (0.1)	0.2 (0.05)
Xylene	0.5 (0.1)	0.2 (0.1)	34.0 (25.0)[a,b]
Xylene + LCr	0.5 (0.1)	BD	0.1[e]
Xylene + HCr	0.5 (0.1)	BD	BD

[a] Significantly more copies than at time 0 ($P = 0.05$).
[b] Significantly more copies than measured in the no-substrate control microcosm at that time ($P = 0.05$).
[c] Treatment microcosms received 3,000 $\mu g\ g^{-1}$ of xylene, low lead (LPb) at 3,000 $\mu g\ Pb^{6+}\ g^{-1}$ soil, high lead (HPb) at 10,000 $\mu g\ g^{-1}$, low chromium at 10 $\mu g\ Cr^{6+}\ g^{-1}$ soil (LCr), or high chromium at 18 $\mu g\ Cr^{6+}\ g^{-1}$ (HCr).
[d] BD, below detection limit (200 copies per reaction mixture). Numbers in parentheses are standard deviations ($n = 3$).
[e] The PHE gene was detected in only one microcosm of three replicates.

TABLE 3. Summary of sequences of cloned bands from DGGE profiles of xylene- and high-chromium-amended microcosms on day 31 (clones starting with "X") and glucose-amended microcosms on day 31 (clones starting with "G")

Clone[a]	Accession no. of clone sequence	Closest GenBank match	Accession no. of GenBank match	Similarity (no. of identical nucleotides/ total no. [%])	Phylogenetic clade
XHCR1(a)[b]	DQ016373	Uncultured actinobacterium	AY217495	177/179 (98)	*Actinobacteria*
XHCR2(a)[b]	DQ016374	*Rhodococcus rhodochrous* DSM 43241	X79288	175/177 (98)	*Actinobacteria*
XHCR3(b)	DQ016375	Bacterium Ellin347	AF498729	176/177 (99)	*Actinobacteria*
XHCR4(c)[b]	DQ016376	*Nocardioides* sp. strain JS884	AF465213	183/186 (98)	*Actinobacteria*
XHCR5(c)[b]	DQ016377	*Rhodococcus ruber* M2	AY247275	175/177 (98)	*Actinobacteria*
XHCR6(d)[b]	DQ016378	*Arthrobacter* sp. strain SMCC G982	AF197037	175/177 (98)	*Actinobacteria*
XHCR7(d)[b]	DQ016379	Earthworm bacterium B37D1	AY039453	176/177 (99)	*Actinobacteria*
XHCR8(e)	DQ016380	*Brevibacterium* sp. strain BN53-1	AB066340	198/198 (100)	*Firmicutes*
XHCR9(f)	DQ016381	*Bacillus niacini* SAFN-021	AY167809	190/197 (96)	*Firmicutes*
XHCR10(g)	DQ016382	*Pseudomonas* sp. strain AEBL3	AY247063	197/197 (100)	γ-*Proteobacteria*
G11(h)	DQ016383	*Arthrobacter globiformis* SAFR-004	AY167856	177/177 (100)	*Actinobacteria*
G12(i)	DQ016384	*Phenylobacterium lituiforme* Fail3	AY534887	172/172 (100)	α-*Proteobacteria*
G13(j)	DQ016385	*Pseudomonas* sp. strain GOBB3-106	AF321011	197/197 (100)	γ-*Proteobacteria*
G14(j)	DQ016386	Proteobacterium 5S2.G8	AY043560	195/197 (98)	β-*Proteobacteria*

[a] The letters in parentheses refer to specific bands labeled in Fig. 5.
[b] Amplicons with the same letter code migrated to the same location in a 35 to 58% denaturing gradient. However, two distinct bands were resolved in narrower (35 to 45% or 45 to 58%) gradients of denaturant, and the bands were excised from that gel.

Phylogenetic identity of dominant phylotypes. Two approaches were used to determine the identity of organisms that became dominant in the microcosms. A number of xylene-degrading bacteria were selected from the microcosm with xylene and high Cr(VI) (F. Beasley et al., manuscript in preparation). Based on an analysis of their 16S rRNA gene sequences, the isolates fell into the following three genera: group I, *Arthrobacter*; group II, *Pseudomonas*; and group III, *Rhodococcus*. Representatives of each group were compared to the original microcosm community by PCR-DGGE. The group I amplicons (*Arthrobacter*) migrated the same distance on the DGGE gel and corresponded to one of the intense bands observed in the microcosm from which they was isolated (Fig. 5D, arrowhead). This band was also common to many of the community profiles from other microcosms (Fig. 5, arrowheads). Group II was also represented by one PCR-DGGE band that was found in the community profiles of microcosms with xylene. There were two PCR-DGGE bands with slightly different migration distances for group II isolates (Fig. 5); however, neither corresponded to a band in the microcosm community profiles.

For bacteria that became dominant in response to the addition of xylene and high Cr(VI) but that were not cultured (Fig. 5D), the DNA from the prominent DGGE band was cloned and sequenced. Ten bands were sequenced; similarities of 98 to 100% to sequences in the database were generally found for the ca. 200 bp that were sequenced (Table 3). Eight of the 10 sequences had the best matches to organisms in the *Actinomycetales*—3 to bacteria in the genus *Arthrobacter*, 3 to *Rhodococcus*, and 1 each to *Nocardiodes* and *Brevibacillus*. The other two sequences best matched those in a *Bacillus* and a *Pseudomonas* species.

Six bands that became dominant in microcosms that were treated with glucose only were sequenced to determine which phylotypes were selected under those conditions. Three of the six matched sequences from the *Actinomycetales*—one each

from the genera *Arthrobacter*, *Nocardiodes*, and *Streptomyces*. The other three sequences originated from the *Proteobacteria*.

DISCUSSION

Microcosms were used to gain a greater understanding of the effects of heavy metals on microbial communities from an environment with a long history of contamination with not only metals, but also aromatic pollutants. Due to simultaneous inputs of pollutants, in situ analysis cannot distinguish the effects of metals from those of aromatic compounds. The experimental design presumed that organic C alone was a strong selective force on community composition; the addition of either glucose or xylene alone changed the communities and reduced diversity by the selection of a small number of organisms—three to five sharp distinct bands arose on 16S rRNA PCR-DGGE fingerprints in addition to a number of fainter bands. However, the addition of organic carbon is necessary as a driving force for community change, and little alteration will be observed in its absence. The fundamental issue addressed here was the further impact of Pb and Cr(VI) on the structure of bacterial communities.

By using a polyphasic approach, we were able to demonstrate that despite the acute inhibitory effects of Pb and Cr on microbial carbon mineralization and net biomass accumulation, there were dynamic changes in the microbial communities. The dynamics are illustrated by the changes in 16S rRNA DGGE fingerprints (Fig. 5 to 7), increases in BPH4 and PHE gene copy numbers (Tables 1 and 2), and increases in culturable metal-resistant bacteria (Fig. 4). All of these changes must result from the proliferation of specific microbes under specific selective conditions.

The most striking conclusion regarding community-wide changes upon metal stress was that their nature was characteristic of the stimulatory carbon source rather than the specific metal added. Thus, glucose-amended microcosms experienced

more sweeping replacements of community members in response to metal additions than did xylene-amended ones. The number of different organic substrates and metals tested was small; however, this result may reflect the distinction between cases where there are large numbers of organisms that might be recruited (glucose catabolizers) and those (xylene) where potential responders (and their levels of metal resistance) are more limited. The Cr(VI) levels were different for each substrate and were titrated to reduce catabolism by a predetermined value; the amount added to glucose microcosms to reduce activity in the glucose microcosms by 90% [4 mg g^{-1}of Cr(VI)] resulted in no metabolic activity in microcosms with xylene.

This experimental approach allowed us to identify some of the indigenous soil populations that responded to these conditions. Intense bands generally only occurred in 16S rRNA PCR-DGGE profiles for microcosms in which carbon mineralization occurred. We believe these intense bands correspond to organisms that have multiplied at the expense of the added organic substrate and are present as a significant fraction of the total population. This argument is strengthened by the significantly higher copy numbers of the catabolic BPH4 and PHE genes in the microcosms with xylene addition. Furthermore, xylene-degrading bacteria that were isolated from the microcosms contained BPH4 or PHE genes (Beasley et al., in preparation) and corresponded to intense bands in the community PCR-DGGE profiles. Other approaches, such as heavy isotope additions (29, 35), have been suggested as an approach to link populations responsible for functions in soil communities, but the approach used here is much simpler and less expensive and can be used on a broader scale in the field. The combination of PCR-DGGE of 16S rRNA genes with quantitative PCR of functional genes does have limitations because an individual band (organism) is not unequivocally linked to a specific function and because not all gene variants for specific catabolic functions are known. However, at the field scale, the correlation between stimulation of specific rRNA gene sequences and specific functional genes does provide a good initial basis to stimulate detailed analyses of the consequences of changes in community structure upon community function.

The phylogenetic identity of many of the bacteria selected under these conditions is consistent with in situ analyses of these (21a) and other metal-contaminated soils. The *Actinomycetales* have been reported to be important in metal-impacted soils (18). In cases where glucose only was added or xylene plus Cr(VI) was added, organisms from several genera of the *Actinomycetales* commonly responded to the stimuli.

Although the primary objective of this study was to analyze changes in community composition, activities were monitored to provide some basis for understanding community dynamics. In general, activity responses were similar to what has been observed in a number of other microcosm studies (8, 19, 37, 38). In the absence of metals, carbon additions stimulated increases in carbon mineralization, microbial biomass, and the number of culturable bacteria. Heavy metals generally suppressed these community responses, as lower carbon mineralization rates and longer lag phases were observed. On a molar basis, Cr was more toxic than Pb; this may reflect its greater mobility and bioavailability in soil (34). In addition, heavy metals inhibited the xylene-degrading community at lower con-

centrations than those required when glucose was the added energy source. As noted above, this difference may reflect the narrower pool of metal-tolerant species that could catabolize xylene than of those that could catabolize glucose.

A final physiological consequence of metal addition was the reduction in net biomass increases at the expense of added organic carbon. As noted above, growth dynamics were still present to produce changes in DGGE fingerprints, culturable bacterial numbers, and catabolic gene copies. However, the lack of biomass increase may also reflect an energy expenditure to implement metal tolerance, as is true in the case of ATP-dependent efflux systems (43). The ratio of mineralized to assimilated organic C was found to increase in other metal-contaminated soils (6), which is consistent with the increased energy expenditure under these conditions.

The BPH4-type biphenyl dioxygenase and PHE genes were routinely detected in control microcosms and most xylene-amended microcosms, rather than the xylene monooxygenase and toluate or benzoate dioxygenases usually associated with xylene metabolism (The University of Minnesota Biocatalysis/Biodegradation Database [http://umbbd.ahc.umn.edu/]). The presence of aromatic oxygenase genes in the control microcosms was not unexpected because the soil sample was taken from a site contaminated with aromatic hydrocarbons. BPH4 and PHE gene copies increased in xylene microcosms and corresponded to changes in CO$_2$ evolution, and in some cases, biomass; this suggests that there was an enrichment of strains harboring these oxygenase genes. Phenol hydroxylase catalyzes the continued oxidation of hydroxylated intermediates in xylene and toluene catabolism (3) and has been detected in other xylene-amended-microcosm studies (B. Baldwin, personal communication). The selection of BPH4 oxygenase genes following the addition of xylenes may seem counterintuitive; however, previous reports have noted the sequence similarity and functional overlap of biphenyl and alkyl-benzene dioxygenases, including toluene dioxygenase (17, 44). The BPH4 subfamily of biphenyl dioxygenase genes, in particular, is closely related to isopropylbenzene dioxygenase genes.

Although Cr(VI) inhibits microbes, there are biotic and abiotic detoxification mechanisms in soil (4). One biotic mechanism (under both aerobic and anaerobic conditions) occurs via Cr(VI) reduction to less toxic and less mobile Cr(III) (14, 48). Cr(VI) reduction to nontoxic levels could have been a precondition for the onset of microbial activity in the microcosms. However, this was not the case in systems to which glucose was added; these could tolerate relatively large additions of Cr(VI), and microbes were mineralizing glucose when most of the Cr(VI) remained. In the case of xylene amendments, the relationship is less clear. Because only low levels of Cr(VI) could be added to retain any xylene degradation at all, even a modest rate of biological reduction resulted in very small residual Cr(VI) concentrations. Coupled with the lag in detectable xylene mineralization even in the absence of Cr(VI), these data do not convincingly show that xylene catabolism occurred while Cr(VI) was present. More sensitive analyses (for example, with radiotracers) would be required to resolve this issue.

Rarefaction analysis of a 16S rRNA gene clone library created from several soils at this site indicated that they contain a relatively low diversity of microbes (21a), and the provision of a single carbon source in microcosms produced a further re-

duction in diversity. These effects are explicable in light of the resource heterogeneity hypothesis (46), i.e., the site is relatively uniformly barren with respect to resource availability due to the lack of plant vegetation. As a result, heterotrophic productivity and diversity are low. The addition of a single C source to microcosms results in even lower organic resource heterogeneity, and there is strong selection for a few types that use that dominant C source. When an additional selection (heavy metals) factor was imposed, the community dynamics were found to be much greater for components expected to contain a large degree of functional redundancy (glucose-catabolizing bacteria) than a more restricted catabolic function (xylene degradation). Consistent with this broader capacity was the greater robustness of glucose catabolism, that is, it recovered and proceeded at much higher metal concentrations than did xylene catabolism.

REFERENCES

1. **Acosta-Martínez, V., Z. Reicher, M. Bischoff, and R. F. Turco.** 1999. The role of tree leaf mulch and nitrogen fertilizer on turfgrass soil quality. Biol. Fert. Soils **29:**55–61.
2. **Altschul, S. F., T. L. Madden, A. A. Schaffer, J. Zhang, Z. Zhang, W. Miller, and D. J. Lipman.** 1997. Gapped BLAST and PSI-BLAST: a new generation of protein database search programs. Nucleic Acids Res. **25:**3389–3402.
3. **Arenghi, F. L. G., D. Berlanda, E. Galli, G. Sello, and P. Barbieri.** 2001. Organization and regulation of *meta* cleavage pathway genes for toluene and *o*-xylene derivative degradation in *Pseudomonas stutzeri* OX1. Appl. Environ. Microbiol. **67:**3304–3308.
4. **Avudainayagam, S., A. Megharaj, G. Owens, R. S. Kookana, D. Chittleborough, and R. Naid.** 2003. Chemistry of chromium in soils with emphasis on tannery waste sites. Rev. Environ. Contam. Toxicol. **178:**53–91.
5. **Baath, E.** 1992. Measurement of heavy metal tolerance of soil bacteria using thymidine incorporation into bacteria extracted after homogenization-centrifugation. Soil Biol. Biochem. **24:**1167–1172.
6. **Baath, E., M. Diaz-Ravina, A. Frostegard, and C. D. Campbell.** 1998. Effect of metal-rich sludge amendments on the soil microbial community. Appl. Environ. Microbiol. **64:**238–245.
7. **Baldwin, B. R., C. H. Nakatsu, and L. Nies.** 2003. Detection and enumeration of aromatic oxygenase genes by multiplex and real-time PCR. Appl. Environ. Microbiol. **69:**3350–3358.
8. **Bardgett, R. D., and S. Saggar.** 1994. Effects of heavy-metal contamination on the short-term decomposition of labeled [C-14] glucose in a pasture soil. Soil Biol. Biochem. **26:**727–733.
9. **Barnhart, C. L., and R. Vestal.** 1983. Effect of environmental toxicant on metabolic activity of natural microbial communities. Appl. Environ. Microbiol. **46:**970–977.
10. **Capone, D. G., D. Reese, and R. P. Kiene.** 1983. Effects of metals on methanogenesis, sulfate reduction, carbon dioxide evolution, and microbial biomass in anoxic salt marsh sediments. Appl. Environ. Microbiol. **45:**1586–1591.
11. **Cassel, D. K., and D. R. Nielsen.** 1986. Field capacity and available water, p. 901–926. *In* A. Klute (ed.), Methods of soil analysis. I. Physical and mineralogical methods, 2nd ed. American Society for Agronomy, Soil Science Society of America, Madison, Wis.
12. **Clesceri, L. S., A. E. Greenberg, and A. D. Eaton.** 1999. Standard methods for examination of water and wastewater, 20th ed. American Public Health Association, Washington, D.C.
13. **Ekschmitt, K., and B. S. Griffiths.** 1998. Soil biodiversity and its implications for ecosystem functioning in a heterogeneous and variable environment. Appl. Soil Ecol. **10:**201–215.
14. **Fein, J. B., D. A. Fowle, J. Cahill, K. Kemner, M. Boyanov, and B. Bunker.** 2002. Nonmetabolic reduction of Cr(VI) by bacterial surfaces under nutrient-absent conditions. Geomicrobiol. J. **19:**369–382.
15. **Feris, K. P., P. W. Ramsey, M. Rillig, J. N. Moore, J. E. Gannon, and W. E. Holbert.** 2004. Determining rates of change and evaluating group-level resiliency differences in hyporheic microbial communities in response to fluvial heavy-metal deposition. Appl. Environ. Microbiol. **70:**4756–4765.
16. **Findlay, R. H.** 1996. The use of phospholipid fatty acids to determine microbial community structure, p. 1–17. *In* A. K. Akkermans, J. D. van Elsas, and F. de Bruijn (ed.), Molecular microbial ecology manual. Kluwer Academic Publishers, Dordrecht, The Netherlands.
17. **Furukawa, K., J. Hirose, A. Suyama, T. Zaiki, and S. Hayashida.** 1993. Gene components responsible for discrete substrate specificity in the metabolism of biphenyl (*bph* operon) and toluene (*tod* operon). J. Bacteriol. **175:**5224–5232.
18. **Gremion, F., A. Chatzinotas, and H. Harms.** 2003. Comparative 16S rDNA and 16S rRNA sequence analysis indicates that Actinobacteria might be a dominant part of the metabolically active bacteria in heavy metal-contaminated bulk and rhizosphere soil. Environ. Microbiol. **5:**896–907.
19. **Gremion, F., A. Chatzinotas, K. Kaufmann, W. V. Sigler, and H. Harms.** 2004. Impacts of heavy metal contamination and phytoremediation on a microbial community during a twelve-month microcosm experiment. FEMS Microbiol. Ecol. **48:**273–283.
20. **Hutchinson, T. C., and M. S. Symington.** 1997. Persistence of metal stress in a forested ecosystem near Sudbury, 66 years after closure of the O'Donnell roast bed. J. Geochem. Explor. **58:**323–330.
21. **Jonas, R. B., C. G. Gilmour, D. L. Stoner, M. M. Weir, and J. H. Tuttle.** 1984. Comparison of methods to measure acute metal and organometal toxicity to natural aquatic microbial communities. Appl. Environ. Microbiol. **47:**1005–1011.
21a. **Joynt, J., M. Bischoff, R. Turco, A. Konopka, and C. H. Nakatsu.** Microbial community analysis of soils contaminated with lead, chromium and petroleum hydrocarbons. Microb. Ecol., in press.
22. **Kamaludeen, S. P. B., M. Megharaj, R. Naidu, I. Singleton, A. L. Juhasz, B. G. Hawke, and N. Sethunathan.** 2003. Microbial activity and phospholipid fatty acid pattern in long-term tannery waste-contaminated soil. Ecotox. Environ. Safety **56:**302–310.
23. **Konopka, A., D. Knight, and R. F. Turco.** 1989. Characterization of a *Pseudomonas* sp. capable of aniline degradation in the presence of secondary carbon sources. Appl. Environ. Microbiol. **55:**385–389.
24. **Konopka, A., T. Zakharova, M. Bischoff, L. Oliver, C. Nakatsu, and R. F. Turco.** 1999. Microbial biomass and activity in lead-contaminated soil. Appl. Environ. Microbiol. **65:**2256–2259.
25. **Konstantinidis, K. T., N. Isaacs, J. Fett, S. Simpson, D. T. Long, and T. L. Marsh.** 2003. Microbial diversity and resistance to copper in metal-contaminated lake sediment. Microb. Ecol. **45:**191–202.
26. **Kozdroj, J., and J. D. van Elsas.** 2001. Structural diversity of microorganisms in chemically perturbed soil assessed by molecular and cytochemical approaches. J. Microbiol. Methods **43:**197–212.
27. **Lane, D. J.** 1991. 16S/23S rRNA sequencing, p. 115–175. *In* E. Stackebrandt and M. Goodfellow (ed.), Nucleic acid techniques in bacterial systematics. John Wiley & Sons, New York, N.Y.
28. **LaPara, T. M., C. H. Nakatsu, L. Pantea, and J. E. Alleman.** 2000. Phylogenetic analysis of bacterial communities in mesophilic and thermophilic bioreactors treating pharmaceutical wastewater. Appl. Environ. Microbiol. **66:**3951–3959.
29. **Manefield, M., A. S. Whiteley, R. I. Griffiths, and M. J. Bailey.** 2002. RNA stable isotope probing, a novel means of linking microbial community function to phylogeny. Appl. Environ. Microbiol. **68:**5367–5373.
30. **Moffett, B. F., F. A. Nicholson, N. C. Uwakwe, B. J. Chambers, J. A. Harris, and T. C. J. Hill.** 2003. Zinc contamination decreases the bacterial diversity of agricultural soil. FEMS Microbiol. Ecol. **43:**13–19.
31. **Muyzer, G., E. C. de Waal, and A. G. Uitterlinden.** 1993. Profiling of complex microbial populations by denaturing gradient gel electrophoresis analysis of polymerase chain reaction-amplified genes coding for 16S rRNA. Appl. Environ. Microbiol. **59:**695–700.
32. **Muyzer, G., S. A. Hottentrager, A. Teske, and C. Wawer.** 1996. Denaturing gradient gel electrophoresis of PCR-amplified 16S rDNA—a new molecular approach to analyse the genetic diversity of mixed microbial communities, p. 1–23. *In* A. Akkermans, J. D. van Elsas, and F. J. de Bruijn (ed.), Molecular microbial ecology manual 3.4.4. Kluwer Academic Publishers, Nowell, Mass.
33. **Nakatsu, C. H., V. Torsvik, and L. Øvreås.** 2000. Soil community analysis using DGGE of 16S rDNA polymerase chain reaction products. Soil Sci. Soc. Am. J. **64:**1382–1388.
34. **Nieboer, E., and A. A. Jusys.** 1988. Biologic chemistry of chromium, p. 21–79. *In* J. O. Nriagu and E. Nieboer (ed.), Chromium in natural and human environments. Wiley, New York, N.Y.
35. **Padmanabhan, P., S. Padmanabhan, C. DeRito, A. Gray, D. Gannon, J. R. Snape, C. S. Tsai, W. Park, C. Jeon, and E. L. Madsen.** 2003. Respiration of ^{13}C-labeled substrates added to soil in the field and subsequent 16S rRNA gene analysis of ^{13}C-labeled soil DNA. Appl. Environ. Microbiol. **69:**1614–1622.
36. **Pielou, E. C.** 1969. An introduction to mathematical ecology. Wiley-Interscience, New York, N.Y.
37. **Rajapaksha, R. M. C. P., M. A. Tobor-Kaplon, and E. Baath.** 2004. Metal toxicity affects fungal and bacterial activities in soil differently. Appl. Environ. Microbiol. **70:**2966–2973.

38. **Renella, G., M. Mench, L. Landi, and P. Nannipieri.** 2005. Microbial activity and hydrolase synthesis in long-term Cd-contaminated soils. Soil Biol. Biochem. **37:**133–139.

39. **Roane, T. M., and S. T. Kellogg.** 1996. Characterization of bacterial communities in heavy metal contaminated soils. Can. J. Microbiol. **42:**593–603.

40. **Said, W. A., and D. L. Lewis.** 1991. Quantitative assessment of the effects of metals on microbial degradation of organic chemicals. Appl. Environ. Microbiol. **57:**1498–1503.

41. **Sambrook, J., E. F. Fritsch, and T. Maniatis.** 1989. Molecular cloning: a laboratory manual. Cold Spring Harbor Laboratory Press, Cold Spring Harbor, N.Y.

42. **Shi, W., M. Bischoff, R. Turco, and A. Konopka.** 2002. Long-term effects of chromium and lead upon the activity of soil microbial communities. Appl. Soil Ecol. **21:**169–177.

43. **Silver, S., and L. T. Phung.** 1996. Bacterial heavy metal resistance—new surprises. Annu. Rev. Microbiol. **50:**753–789.

44. **Smith, M. R., and C. Ratledge.** 1989. Catabolism of biphenyl by *Pseudomonas* sp. NCIB 10643 and *Nocardia* sp. NCIB 10503. Appl. Microbiol. Biotechnol. **30:**395–401.

45. **Stoppel, R. D., and H. G. Schlegel.** 1995. Nickel-resistant bacteria from anthropogenically nickel-polluted and naturally nickel-percolated ecosystems. Appl. Environ. Microbiol. **61:**2276–2285.

46. **Tilman, D.** 1982. Resource competition and community structure. Princeton University Press, Princeton, N.J.

47. **Vives-Rego, J., D. Vaque, and J. Martinez.** 1986. Effect of heavy metals and surfactants on glucose metabolism, thymidine incorporation and exoproteolytic activity in sea water. Water Res. **20:**1411–1415.

48. **Wang, Y. T., and H. Shen.** 1995. Bacterial reduction of hexavalent chromium. J. Ind. Microbiol. **14:**159–163.

49. **Wenderoth, D. F., E. Stackebrandt, and H. H. Reber.** 1999. Metal stress selects for bacterial ARDRA-types with a reduced catabolic versatility. Soil Biol. Biochem. **33:**667–670.